

Supplementary Materials

Organization of Bone Mineral: The Role of Mineral–Water Interactions

Stanislas Von Euw^{1,*,+}, **Tsou-Hsi-Camille Chan-Chang**¹, **Caroline Paquis**¹, **Bernard Haye**¹, **G rard Pehau-Arnaudet**², **Florence Babonneau**¹, **Thierry Azais**¹ and **Nadine Nassif**¹

¹ CNRS, Coll ge de France, Laboratoire de Chimie de la Mati re Condens e de Paris (LCMCP), Sorbonne Universit , 4 place Jussieu, F-75005 Paris, France; tsou.chan_chang@etu.upmc.fr (T.-H.-C.C.-C.); carolinepaquis@gmail.com (C.P.); bernard.haye@upmc.fr (B.H.); florence.babonneau@upmc.fr (F.B.); nadine.nassif@upmc.fr (N.N.); thierry.azais@upmc.fr (T.A.)

² UMR 3528 and UTech UBL, Institut Pasteur, 28 rue du Docteur Roux, 75015 Paris, France ; gerard.pehau-arnaudet@pasteur.fr

* Correspondence: voneuws@tcd.ie

† Current address: Trinity Centre for Bioengineering, Trinity Biomedical Sciences Institute, Trinity College Dublin (TCD), Dublin 2, D02 R590, Ireland.

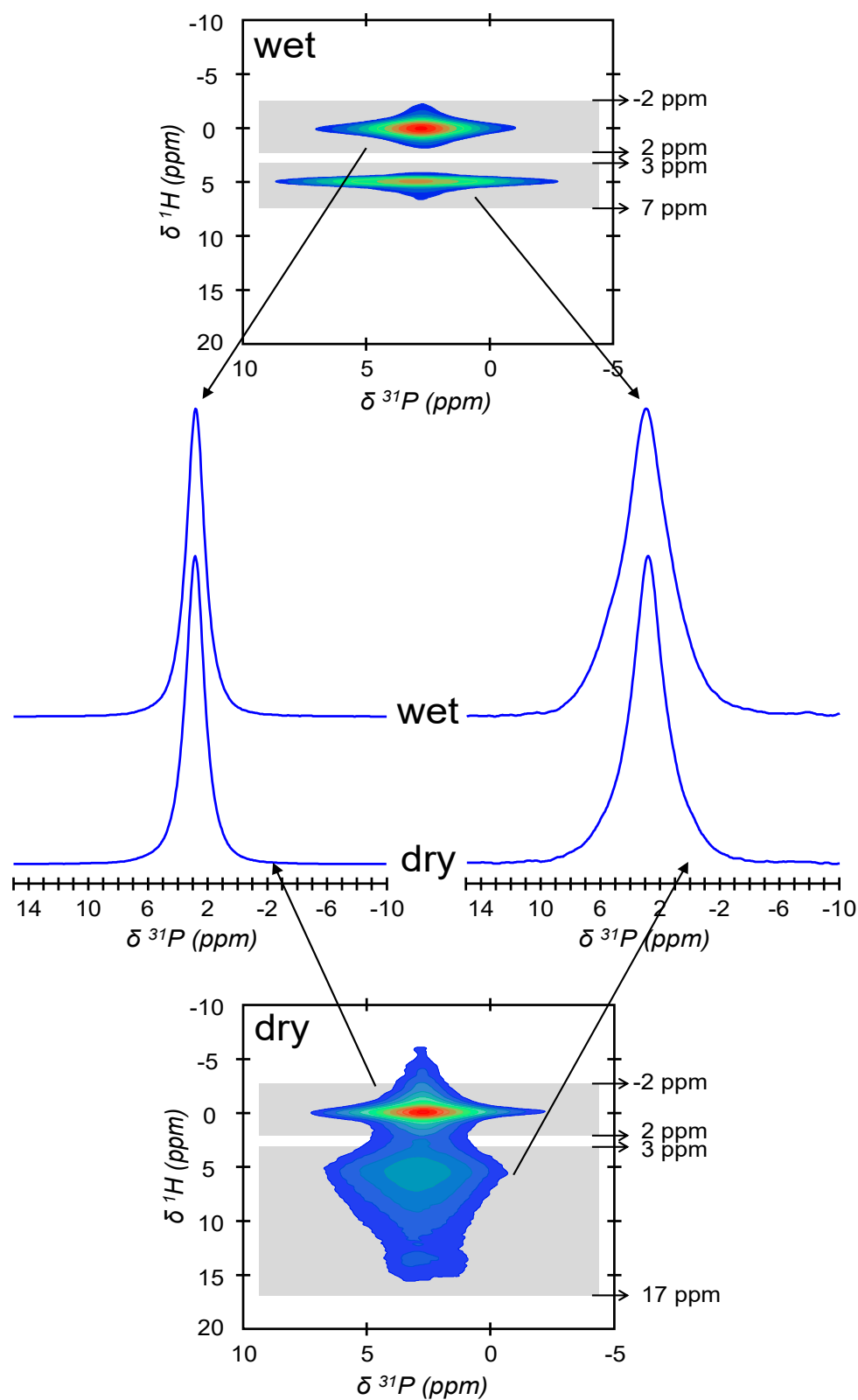


Figure S1. Individual ^{31}P signals of the crystalline nanoparticle core and the amorphous surface layer within bone-like hydroxyapatite particles, together with their evolution from dry to wet conditions. Shown are the normalized one-dimensional (1D) individual ^{31}P NMR signals of the crystalline nanoparticle core (left) and the amorphous surface layer (right) of the synthetic Carbonated HydroxyApatite (CHA) particles in dry conditions (bottom) and soaked in water (top). These individual ^{31}P NMR signals were extracted from the two-dimensional (2D) $\{^1\text{H}\}^{31}\text{P}$ Heteronuclear Correlation (HetCor) NMR spectra that are shown here. The sums of the F2 slices taken at the OH⁻ ions position (from $\delta^1\text{H} = -2$ to 2 ppm) in F1 have been used to generate the individual ^{31}P signals of

the crystalline nanoparticle core both in dry and wet conditions. The sums of the F2 slices taken at the bound water molecules position (from $\delta^1\text{H} = 3$ to 7 ppm) or the residual structural water molecules together with HPO_4^{2-} ions position (from $\delta^1\text{H} = 3$ to 17 ppm) in F1 have been used to generate the individual ^{31}P signals of the amorphous surface layer, respectively in wet and dry conditions.

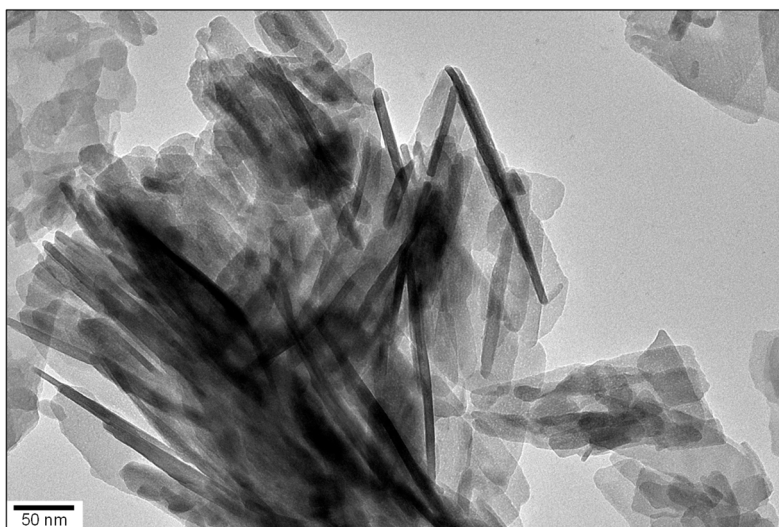


Figure S2. Observations of bone-like platelet-shaped hydroxyapatite particles seen edge-on. Transmission electron micrograph (TEM) of the synthetic Carbonated HydroxyApatite (CHA) particles. Some of them are here standing vertically such that their smallest side faces are exposed while their largest side faces are parallel to the electron beam.

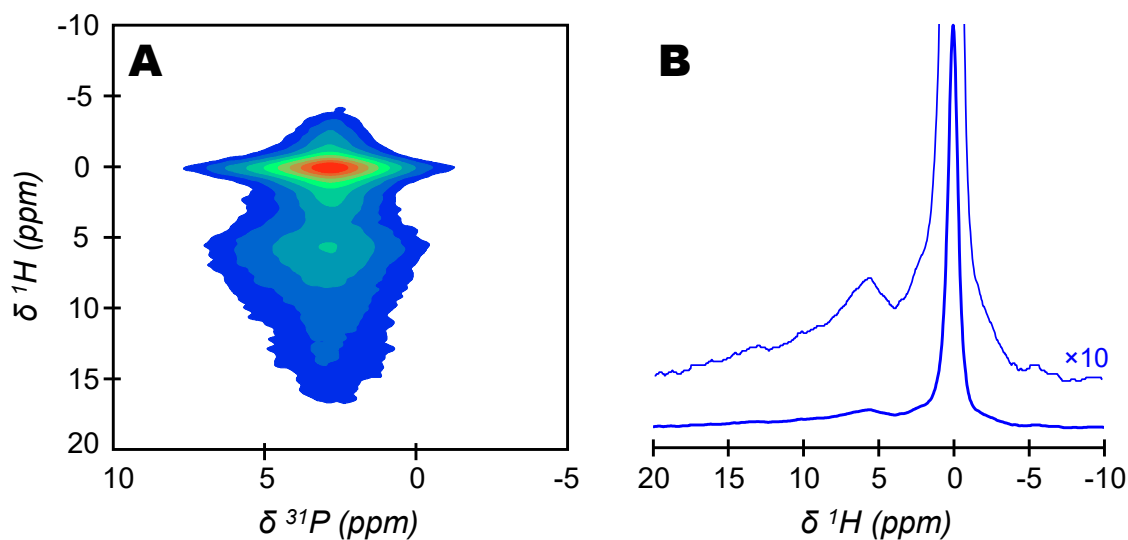


Figure S3. Spatial proximities between phosphorus and hydrogen species within the needle/rod-shaped carbonated hydroxyapatite particles. (A) Two-dimensional (2D) $^1\text{H}/^{31}\text{P}$ Heteronuclear Correlation (HetCor) NMR spectrum of the synthetic needle/rod-shaped Carbonated HydroxyApatite (CHA-needle/rod) sample. Signal intensity increases from blue to red. (B) One-dimensional (1D) ^1H projection of the vertical F1 dimension extracted from the 2D $^1\text{H}/^{31}\text{P}$ HetCor NMR spectrum displayed in (A).

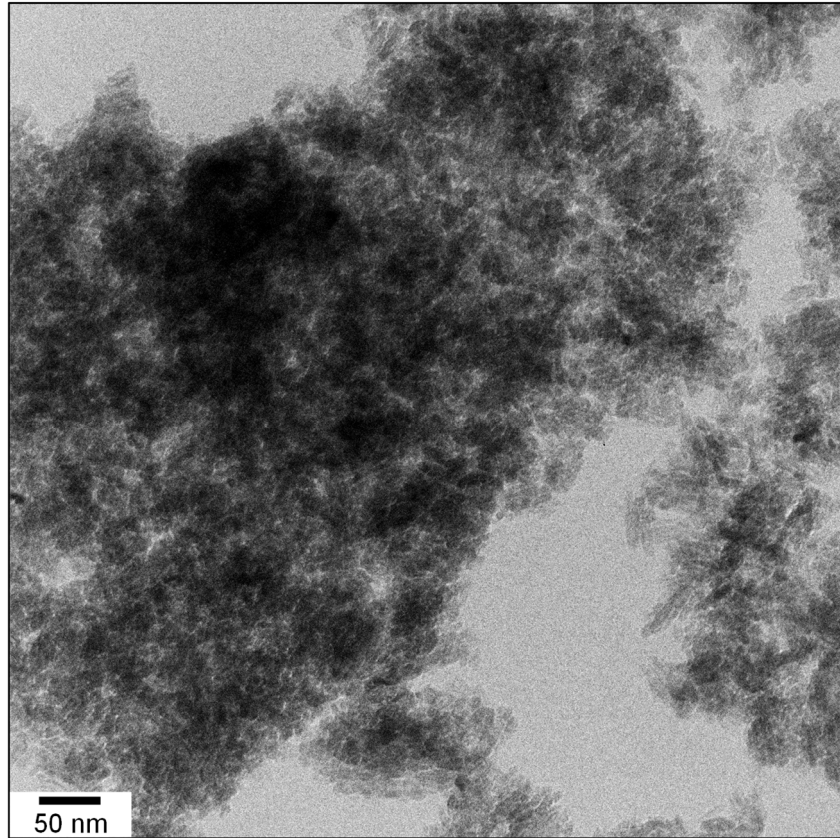


Figure S4. Behavior of the needle/rod-shaped carbonated hydroxyapatite particles in water. Shown is a representative cryogenic transmission electron micrograph (cryo-TEM) of the synthetic needle/rod-shaped Carbonated HydroxyApatite (CHA-needle/rod) particles dispersed in water.

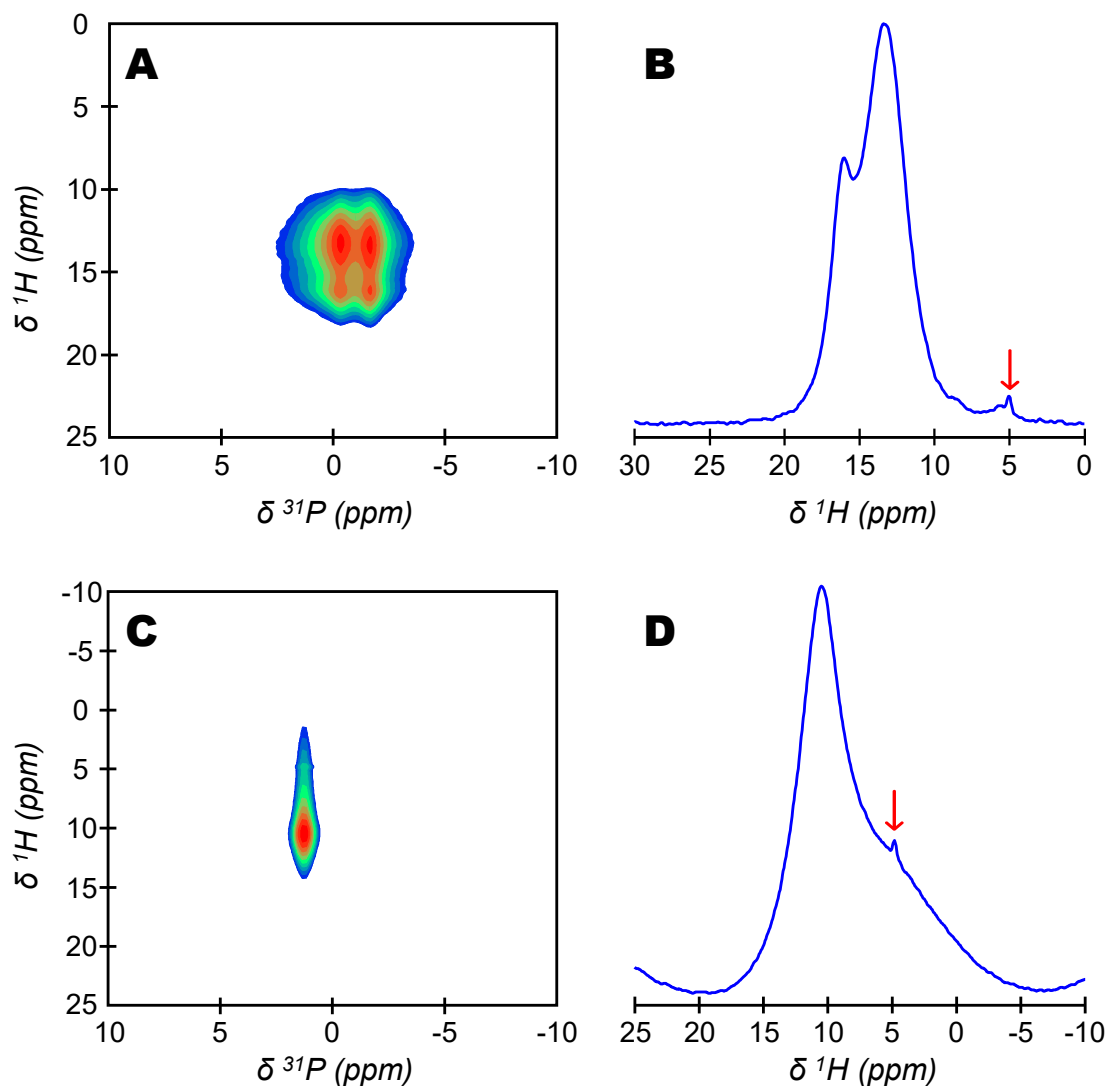


Figure S5. Spatial proximities between phosphorus and hydrogen species within monetite and brushite. Two-dimensional (2D) $\{^1\text{H}\}^{31}\text{P}$ Heteronuclear Correlation (HetCor) NMR spectra of synthetic monetite (A) and brushite (C) samples soaked in water (pH 4). Signal intensity increases from blue to red. Normalized one-dimensional (1D) ^1H projections of the vertical F1 dimensions extracted from the 2D $\{^1\text{H}\}^{31}\text{P}$ HetCor NMR spectra of monetite (B) and brushite (D). For monetite, the spatial proximities among the various ^1H and ^{31}P nuclei in the HPO_4^{2-} ions are detected as two correlation peaks observable at $\delta^{31}\text{P} = -0.2$ and -1.4 ppm in the F2 (^{31}P) dimension, which are both associated with two correlation peaks observable at $\delta^1\text{H} = 13.3$ and 16.1 ppm in the F1 (^1H) dimension. For brushite, the spatial proximities among the various ^1H and ^{31}P nuclei in the HPO_4^{2-} ions are detected as a single correlation peak observable at $\delta^{31}\text{P} = 1.4$ ppm in the F2 (^{31}P) dimension and in the range of $\delta^1\text{H} = 8$ - 15 ppm in the F1 (^1H) dimension. In addition, the structural water molecules present in brushite are detected as a broad correlation peak observable at $\delta^{31}\text{P} = 1.4$ ppm in the F2 (^{31}P) dimension and centered at around $\delta^1\text{H} = 5$ ppm in the F1 (^1H) dimension. Last, the red arrows indicate the presence of tiny signals of bound water which are not observable in dry conditions.